JOURNAL OF MATERIALS SCIENCE 27 (1992) 1913–1925

Polytype distribution in silicon carbide

L. K. FREVEL, D. R. PETERSEN, C. K. SAHA
Dow Corning Corporation, 3901 S. Saginaw Road, Midland, Michigan 48686, USA

Silicon carbide is a candidate material for high-performance applications. It exists as a composite of many structurally distinct but related polytypes with differing physical properties. It is well known, for example, that the flexural strength of formed SiC composites is strongly dependent on the relative amounts of the various polytypes present in the composite. X-ray powder diffraction is the method of choice to determine polytype distribution. Each of the SiC polytypes gives a unique diffraction pattern; unfortunately, the patterns for the various polytypes superimpose in part, making interpretation difficult. The authors have developed a method to separate the superimposed patterns to give quantitative information on the distribution of the polytypes in the composite. This approach provides a useful tool in relating preparation conditions to performance properties.

1. Introduction

Silicon carbide has many polymorphs which are closely related structurally and are designated as polytypes. The crystal structures of these polytypes are based on the tetrahedral coordination of carbon and silicon. The simple structure of SiC [SiC(3C) or β-SiC] is readily understood when viewed as the cubic diamond structure in which every other carbon atom is replaced by a silicon atom. In the diamond structure, each carbon atom is tetrahedrally bonded to the four nearest carbons with adjacent tetrahedral bonds in a 60° staggered conformation (Fig. 1). This staggered conformation corresponds to that of the ethane molecule, for which the barrier to rotation corresponds to 3 kcal mol^{-1}. Fig. 2 depicts the diamond structure as a three-dimensional polymer of carbon. The most dense packing of carbons resides in the puckered layer of completely linked C_6 rings of the chair configuration (as in cyclohexane). Each puckered layer is cross-linked to an equivalent layer above and below. Fig. 3 shows the structure of β-SiC in which the effective covalent radii of carbon and silicon are drawn for only two neighbouring atoms. The difference between the sum of the standard covalent radii for C and Si and the observed Si–C distance is 0.006 nm (0.195–0.189 nm). This small difference indicates predominantly covalent bonding in SiC.

Another simple structure of SiC [SiC(2H)] is likewise viewed as derived from that of lonsdaleite, the hexagonal allotrope of tetrahedrally bonded carbon, in which every other carbon atom is replaced by a silicon atom. Although very closely related to the diamond structure, the structure of the hexagonal allotrope shows adjacent puckered layers bonded in an eclipsed conformation (Fig. 4). Fig. 5 depicts the structure of lonsdaleite, the hexagonal allotrope of tetrahedrally bonded carbon; Fig. 6, the structure of SiC(2H).

The structures of the cubic SiC(3C) and the hexagonal SiC(2H) polytypes differ only in the cross-linking of the identical puckered SiC layers. Since the layers can be bonded in three different manners (arbitrarily designated by Wyckoff [1] as 0, 1, 2) then the

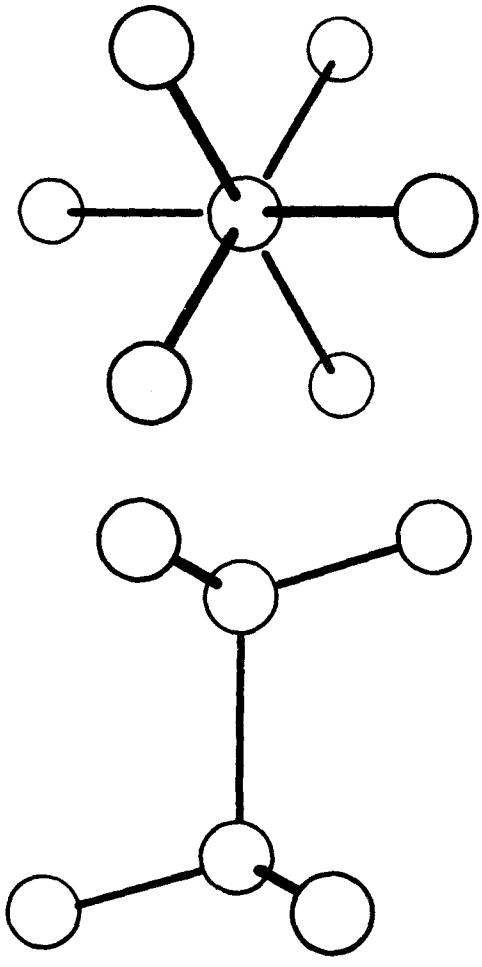

Figure 1 Diamond structure of SiC.

0022–2461

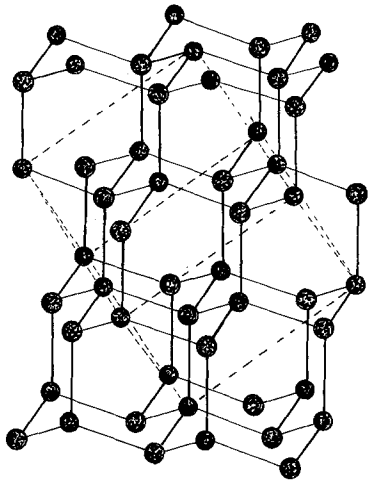

Figure 2 The cubic diamond structure. ●, C.

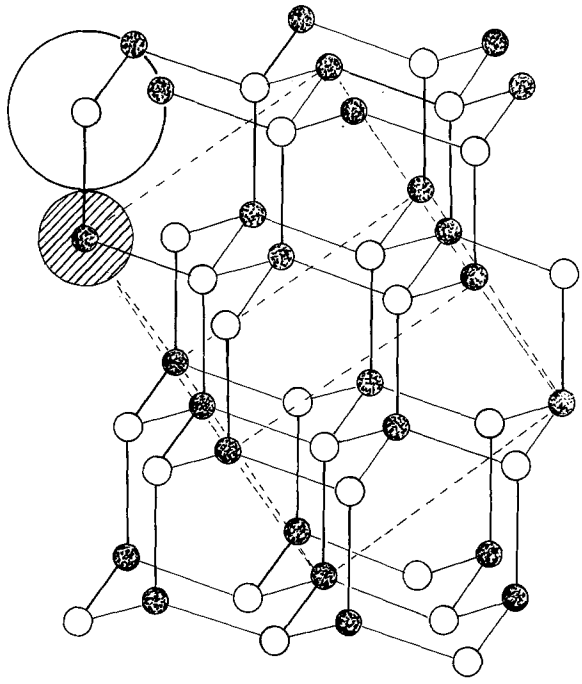

Figure 3 The cubic silicon carbide structure, β-SiC or SiC (3C). ●, C; ○, Si.

bonding sequence in SiC(3C) corresponds to 0, 1, 2 . . . and in SiC(2H) corresponds to 0, 1 . . . The many other polytypes of SiC can be interpreted as regularly repeated mixed sequences of β-SiC and SiC(2H).

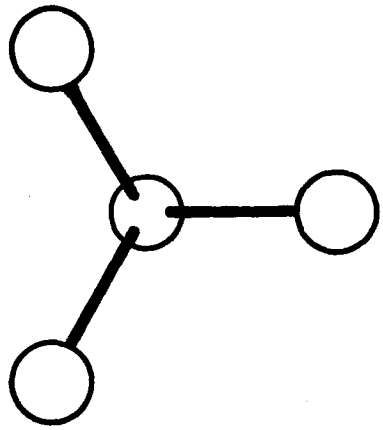

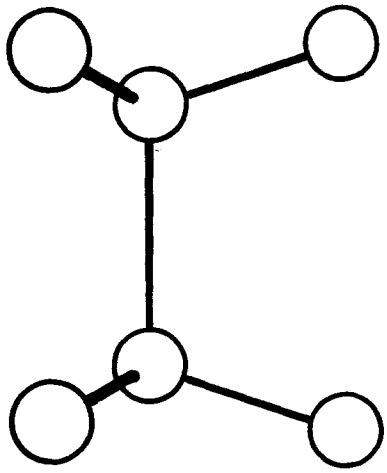

Figure 4 The hexagonal allotrope of tetrahedrally bonded carbon.

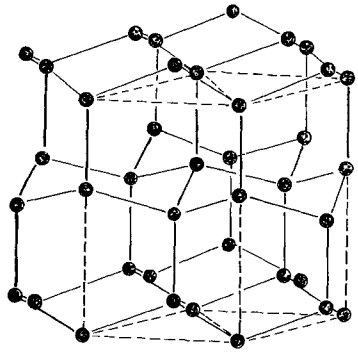

Figure 5 The hexagonal lonsdaleite structure. ●, C.

2. Powder patterns of the more common polytypes of SiC

The simplest powder pattern of SiC is that of β-SiC (see Table I). Table II reproduces the calculated pattern of SiC(2H) as well as the calculated relative peak heights and relative integrated intensities. For SiC(4H), the observed d and I values are given by PDF 22-1317 and the calculated pattern by PDF 29-1127. Likewise, for SiC(6H) the experimental data and the corresponding calculated data are found in PDF 29-1131 and PDF 29-1128. Tables III–VII, in ascending order of complexity, reproduce the powder data of other common polytypes of SiC.

The calculated patterns were generated from the POWD12 computer program [2], which can generate diffractograms of multiphase mixtures of SiC polytypes. Input data consist of respective weight percentages, the respective crystallite sizes, and the type of profile shape of a diffraction peak.

Fig. 7 shows a calculated diffractogram of β-SiC for 30-nm crystallites and a pseudo-Voigt peak profile (see also Table I). Fig. 8 shows the diffractogram for

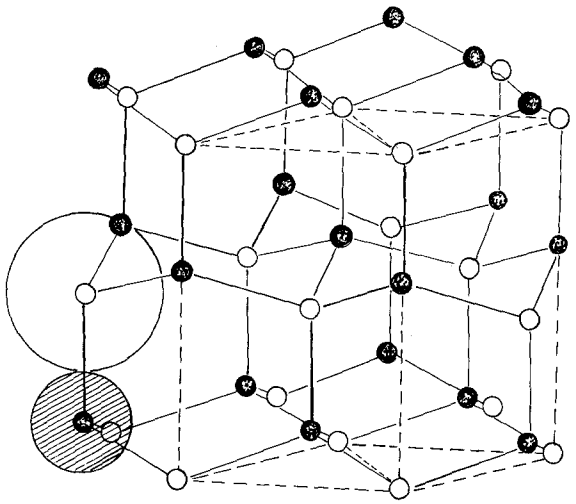

Figure 6 The hexagonal silicon carbide structure SiC(2H). ●, C; ○, Si.

TABLE I β-SiC, 2,2F$\bar{4}$3m(4)[a]; PDF[b] 29-1129. Calculated powder pattern based on $a_c = 0.43593(6)$ nm, $z_c = 4$SiC.

d_{obs} (nm)	$10^2\ (I/I_1)_{obs}$	hkl	d_{calc} (nm)	$10^2\ (I/I_1)_{calc}$
0.252	100	111	0.2517	100
0.218	20	200	0.2180	19
0.1541	35	220	0.15412	43
0.13140	25	311	0.13144	27
0.12583	5	222	0.12584	4
0.10893	5	400	0.10898	4
0.09999	10	331	0.10001	7

[a] Structure classification for β-SiC [11].
[b] PDF = Powder Diffraction File (International Centre for Diffraction Data, Swarthmore, PA).
Shortest bond = $s_{c-Si} = a3^{1/2}/4 = 0.1888(1)$ nm.
All bond angles are tetrahedral, namely 109.471°.
The smallest unit cell for β-SiC can be expressed as a rhombohedral cell: $a_r = a_c/2^{1/2} = 0.30825$ nm and $\alpha = 60°$, containing one SiC.

TABLE II SiC(2H), 2,2P6$_3$mc(2), PDF 29-1130, PDF 29-1126-C. Calculated powder pattern based on $a_h = 0.3081$ nm, $c_h = 0.5031$ nm (single crystal data); $z = 2$SiC.

d_{obs} (nm)	$10^2\ (I/I_1)^a_{obs}$	hkl	d_{calc} (nm)	$10^2\ (I/I_1)_{calc}$
0.267	75	100	0.2668	79
0.252[b]	50[c]	002	0.2516	51
0.236	100	101	0.2357	100
0.183	25	102	0.1830	24
0.154	23[c]	110	0.1541	37
0.143	50	103	0.1420	34
0.133	10	200	0.1334	5
0.131	10[c]	112	0.1314	24
0.129	20	201	0.1290	11
0.126	2[c]	004	0.1258	2
0.118	10	202	0.1179	4

[a] I/I_1 = relative peak intensity, referred to the most intense diffraction peak.
[b] Underlined d-spacings overlap d-spacings of β-SiC.
[c] $I_{(\beta-SiC)}$ subtracted.
Synthesized from mixture of ($CH_3SiCl_3 + H_2$) in graphite crucible at ~ 1400–1460 °C. A powder pattern completely free at β-SiC could not be obtained [12].

30-nm crystallites of β-SiC. Note that the three strongest peaks are still appearing at the expected 2θ values. However, the 2 0 0 reflection becomes an inflection on the strong 1 1 1 peak. Patterns of this type have been observed for Nicalon. Fig. 9 pertains to the calculated diffractogram of SiC(6H) (see also Table III).

If one now generates a diffractogram (Fig. 10) of a 50/50 mixture of SiC(6H) and SiC(3C), each 30 nm, one is surprised at the low relative intensities of the five unambiguous reflections of SiC(6H). Obviously, if the crystallite size of SiC(6H) were less than 10 nm, there would be serious difficulty in detecting SiC(6H) at the 50% level. However, for well-crystallized SiC(6H), the intensities of the unambiguous reflections can be measured by careful step-scanning. Then by calculating the ratio of the observed intensities to the corresponding reflections of 100% SiC(6H), a scale factor for calculating the contribution of SiC(6H) to the superposed reflections can be calculated. Summing the intensities of the observed unambiguous reflections and the calculated contributing intensities to the superposed reflections and then dividing this sum by the sum of all the observed intensities (above background), the weight fraction of SiC(6H) in the mixture is obtained. The quantitative determination of the weight fraction of a particular polytype is based on the premise that the total integrated intensity of the scattered X-rays from 0 to 180° (2θ) is the same for all SiC polytypes. Several examples of this type of quantitative analysis of SiC polytypes will be cited below.

Continuing with the calculated powder patterns of the common polytypes, one notices the increasing number of peaks in the region from 30–45° (2θ) for Cu$K\alpha$ radiation (Table VIII).

For accurate resolution of phases in multiphase mixtures of SiC polytypes, one should carefully step-scan (with narrow slits) the 30–45° (2θ) interval in order to obtain useful profile data revealing non-uniform broadening of peaks or asymmetrical broadening of overlapping peaks. The presence of broad asymmetrical undulations in the background intensity usually reveals a non-crystalline component.

Another type of profile broadening arises from disorder in the regular sequences of puckered SiC layers. However, not all reflections are broadened uniformly. If the various polytypes are described in terms of comparable hexagonal unit cells (see Tables III and VI) [1] one notes the same value of $a_0 = 0.3080$ nm for all SiC polytypes and $c_0 = 0.252 \times z$ nm, where z is equal to the number of SiC per unit cell. For all polytypes, the ($h\,k\,0$) reflections remain sharp; whereas (1 0 l) reflections are broadened with increasing randomness in the sequences of layers, but non-uniformly with specific values of z. Elaborate theoretical expressions for the intensity profiles of disordered structures have been derived [3–5].

3. Quantitative analysis of mixtures of silicon carbide polytypes

Over the past 4 years, the authors have obtained samples of purportedly pure SiC(6H) and β-SiC; but

TABLE III SiC(6H), 2,2P6$_3$mc(6), PDF 29-1131. Calculated powder pattern based on $a_h = 0.30817$ nm, $c_h = 1.51183$ nm

d_{obs} (nm)	$10^2(I/I_1)_{obs}$	hkl	d_{calc} (nm)	Integrated $10^2(I/I_1)_{calc}$	Peak $10^2(I/I_1)_p$
0.2621	40	101	0.2628	54	33
0.2511	100	006	0.2520	67	100
		102	0.2517	100	
0.2352	20	103	0.2359	63	37
0.2174	10	104	0.2180	27	15
		105	0.2001	11	6
		107	0.1679	18	7
0.1537	35	108	0.15423	48	52
		110	0.15409	96	
0.1418	15	109	0.14216	47	14
		201	0.13292	10	
		1010	0.13154	21	33
0.1311	40	116	0.13145	84	
		202	0.13141	21	
0.1286	15	203	0.12900	17	5
		0012	0.12599	6	4
0.1256	7	204	0.12583	9	
		1011	0.12219	4	2
		205	0.12208	4	
		207	0.11352	7	1
0.1087	15	208	0.10901	21	3
		1013	0.10661	3	nil
0.1042	7	209	0.10449	24	3
		211	0.10065	12	
0.1004	15	1014	0.10010	13	6
		2010	0.10004	13	
		212	0.09999	25	

TABLE IV SiC(8H), 2,2P6$_3$mc(8). Calculated powder pattern based on single crystal data: $a_h = 0.3079$ nm; $c_h = 2.0147$ nm.

d_{calc} (nm)	$10^2(I/I_1)_{peak}$	hkl_l
0.2666	11	100_7
0.2643		101_6
0.2578	84	102
0.2518	77	008
0.2478	100	103
0.2357	26	104
0.2224	28	105
0.2088	12	106
0.19560	1	107
0.18309	2	108
0.17145	1	109
0.16075	13	1·0·10
0.15395	37	110
0.15097	18	1·0·11
0.14208	6	1·0·12
0.13399	7	1·0·13
0.13332	nil	200
0.13303	nil	201
0.13217		202_8
0.13135	23	118_{49}
0.13077		203_{12}
0.12889	2	204_4
0.12664		$1·0·14_5$
0.12658	4	205_6
0.12592		$0·0·16_4$
0.12391	1	206

only β-SiC from Superior Graphite Company was found to be phase-pure. Several examples are cited below to illustrate the phase identification of 'pure' SiC samples.

SiC (Cerac pure; lot 1587) was analysed by the method described above and found to contain 86.3 wt% SiC(6H) and 11.3 wt% SiC(15R). Columns 1 and 2 of Table IX reproduce the experimental diffraction data obtained with Cu$K\alpha$ radiation (40.0 kV, 20.0 mA; graphite monochromator for diffracted beam). Columns 3 and 4 list the matched d-spacings (d_s; nm) and the corresponding intensities (I_s, arbitrary units). Columns 6 and 7 give corresponding data for the calculated pattern of SiC(6H). The last column expresses the residual intensities. For example, the strongest reflection 0.2521 nm (130) is fully accounted for: 130 − 125 − 5.1 = −0.1. The faint, unassigned reflections 0.2730, 0.1610 and 0.1505 nm pertain to one or more minor impurities. The weight percentage of SiC(6H) is obtained by summing I_s(SiC(6H)) of column 4 and dividing this sum by I_v(SiC) = 454; i.e. 395/454 = 87.0% SiC(6H). If we use the calculated values of (I_s) in column 7 then $\Sigma\{I_s[\text{SiC(6H)}]\}$ = 388.6 and the wt% SiC(6H) is 85.6%. (Note that the weak permissible reflections at 0.2001 and 0.1679 nm were observed but were missed in PDF 29-1131.) For SiC(15R) the corresponding analyses yielded 11.6 and 10.9 wt%. Thus the assay for SiC ranges from 96.5 to 98.6%. The presence of minor (~5%) concentrations of SiC(4H) could not be ruled out in view of overlapping reflections at 0.2666 and 0.2574 nm. However, the combined concentrations of SiC(15R) and SiC(4H) would be ~12 wt%.

Another sample of pure silicon carbide was obtained from the National Bureau of Standards. This standard sample SRM 112 had the following certified

TABLE V SiC(15R), 2,2R3m(5), PDF 22-1301. Calculated powder pattern based on $a_h = 0.3079$ nm, $c_h = 3.778$ nm.

d_{obs} (nm)	$10^2(I/I_1)_{visual}$	hkl	d_{calc} (nm)	$10^2(I/I_1)_p$	$10^2(I/I_1)_i$
0.266	40	101, 012	0.2660, 0.2640	34	12, 42
0.258	80	104	0.2566	71	100
0.251	80	0·0·15, 015	0.2518, 0.2515	100	98, 47
0.240	70	107	0.2391	49	74
0.232	60	018	0.2322	34	53
0.219	10	1010	0.2178	7	11
0.211	30	0111	0.2106	11	18
0.197	10	1013	0.1965	4	7
		0114	0.1897		2
		10·16	0.1768	1	2
0.170	20	0117	0.1708	4	9
0.159	60	1·019	0.1594	11	26
0.154	100	0·1·20. 110	0.1541, 0.1540	40	14, 88
0.1444	60	1·0·22	0.1444	11	31
0.1398	40	0·1·23	0.1398	8	25
		021, 202	0.1333, 0.1332		1, 4
0.1320	20	024, 1·0·25	0.1320, 0.1315	23	10, 5
0.1311	90	1·1·15, 205	0.1314, 0.1313		66, 5
0.1297	20	027	0.1294	3	10
0.1281	20	208, 0·1·26	0.1283, 0.1276	3	8, 7
0.1257	20	0·0·30, 0·2·10	0.1259, 0.1257	2	5, 2
0.1246	10	2·0·11	0.1243		4
		0·2·13, 1·0·28	0.1212, 0.1204	nil	1
		2·0·14	0.1195	nil	nil
		0·2·16	0.1161	nil	1
0.1143	10	2·0·17	0.1143	nil	2
0.1106	30	1·0·31, 0·2·19	0.1108, 0.1107	1	8, 4

TABLE VI SiC(21R), 2,2R3m(7), PDF 22-1319. Calculated powder pattern based on $a_h = 0.3079$ nm; $c_h = 5.289$ nm

d_{obs} (nm)	$10^2(I/I_1)_{visual}$	hkl	d_{calc} (nm)	$10^2(I/I_1)_p$	$10^2(I/I_1)_i$
		101	0.2663	8	3
		012	0.2653		12
0.263	70	104	0.2614	21	37
		015	0.2586	27	48
0.253	100	0·0·21	0.2518	100	100
		107	0.2515		97
0.247	20	018	0.2473	28	51
0.240	20	1·0·10	0.2381	19	37
0.235	10	0·1·11	0.2332	14	29
0.223	10	1·0·13	0.2231	8	17
0.217	10	0·1·14	0.2178	11	23
		1·0·16	0.2075	3	8
0.201	30	0·1·17	0.2025	3	6
		1·0·19	0.1926	1	2
		0·1·20	0.1878	nil	1
		1·0·22	0.1786	nil	1
		0·1·23	0.1742	1	2
0.166	10	1·0·25	0.1657	3	8
0.162	10	0·1·26	0.1617	3	12
		1·0·28	0.1541	31	29
0.154	80	110	0.1540		89
0.151	20	0·1·29	0.1505	5	17
0.1442	30	1·0·31	0.1437	4	16
0.1407	20	0·1·32	0.1405	3	14
0.1337	10	1·0·34	0.1344	2	9
		202	0.1332	nil	1
		024	0.1327	2	4
		205	0.1323		5
0.1311	70	0·1·35	0.1315	16	11
		1·1·21	0.1314		67
		027	0.1313		11
		208	0.1307		6
0.1293	10	0·2·10	0.1293	1	5

TABLE VII SiC(33R), 2,2R3m(11), PDF 22-1316. Calculated powder pattern based on a_h = 0.3079 nm; c_h = 8.311 nm

d_{obs} (nm)	$10^2(I/I_1)_{visual}$	hkl	d_{calc} (nm)	$10^2(I/I_1)_p$	$10^2(I/I_1)_i$
		101	0.2665		2
		012	0.2661		1
		104	0.2645		13
0.263	50	015	0.2633	31	40
		107	0.2602		29
		018	0.2583		2
0.253	100	1·0·10	0.2539	100	63
		0·0·33	0.2518		100
		0·1·11	0.2515		62
		1·0·13	0.2461	9	14
		0·1·14	0.2433		1
0.238	60	1·0·16	0.2373	29	52
		0·1·17	0.2341	26	45
		1·0·19	0.2277	3	1
		0·1·20	0.2245		5
0.218	30	1·0·22	0.2178	7	15
		0·1·23	0.2145	6	13
0.209	20	1·0·25	0.2080	2	0
		0·1·26	0.2048		5
0.200	20	1·0·28	0.1982	3	6
		0·1·29	0.1952	1	2
		1·0·37	0.1718	1	3
0.169	20	0·1·38	0.1691	3	8
0.164	20	1·0·40	0.1639	2	7
0.156	30	1·0·43	0.1565	6	18
0.154	80	0·1·44	0.1541	34	18
		110	0.1540		89
0.1497	10	1·0·46	0.1496	2	5
		0·1·47	0.1474	nil	1
0.1434	30	1·0·49	0.1431	6	23
0.1410	30	0·1·50	0.1411	6	21
		0·1·53	0.1352	1	3
		024	0.1331		1
		205	0.1329		4
		027	0.1325		3
		0·2·10	0.1317		7
		1·0·55	0.1315		7
0.1313	70	1·1·33	0.1314	20	67
		2·0·11	0.1313		7
		0·2·13	0.1305		2

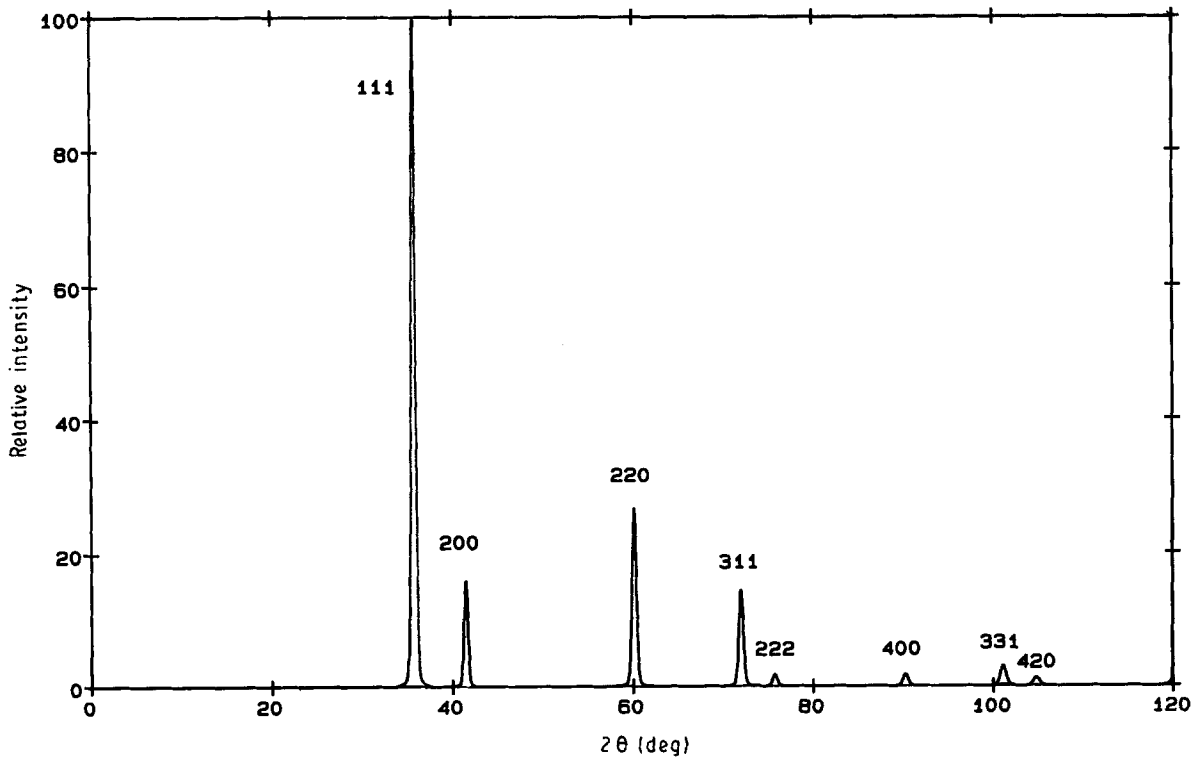

Figure 7 Calculated X-ray diffraction pattern SiC(3C), mean crystallite diameter 30 nm.

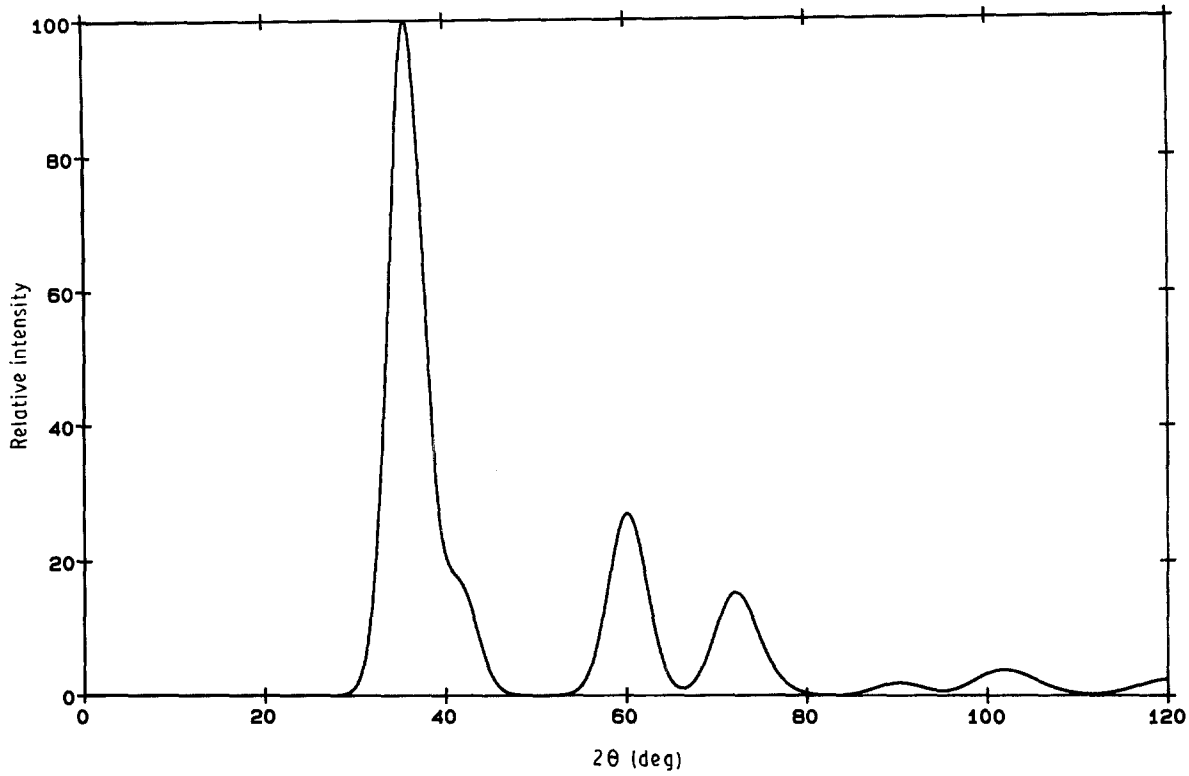

Figure 8 Calculated X-ray diffraction pattern for SiC(3C), mean crystallite diameter 3 nm.

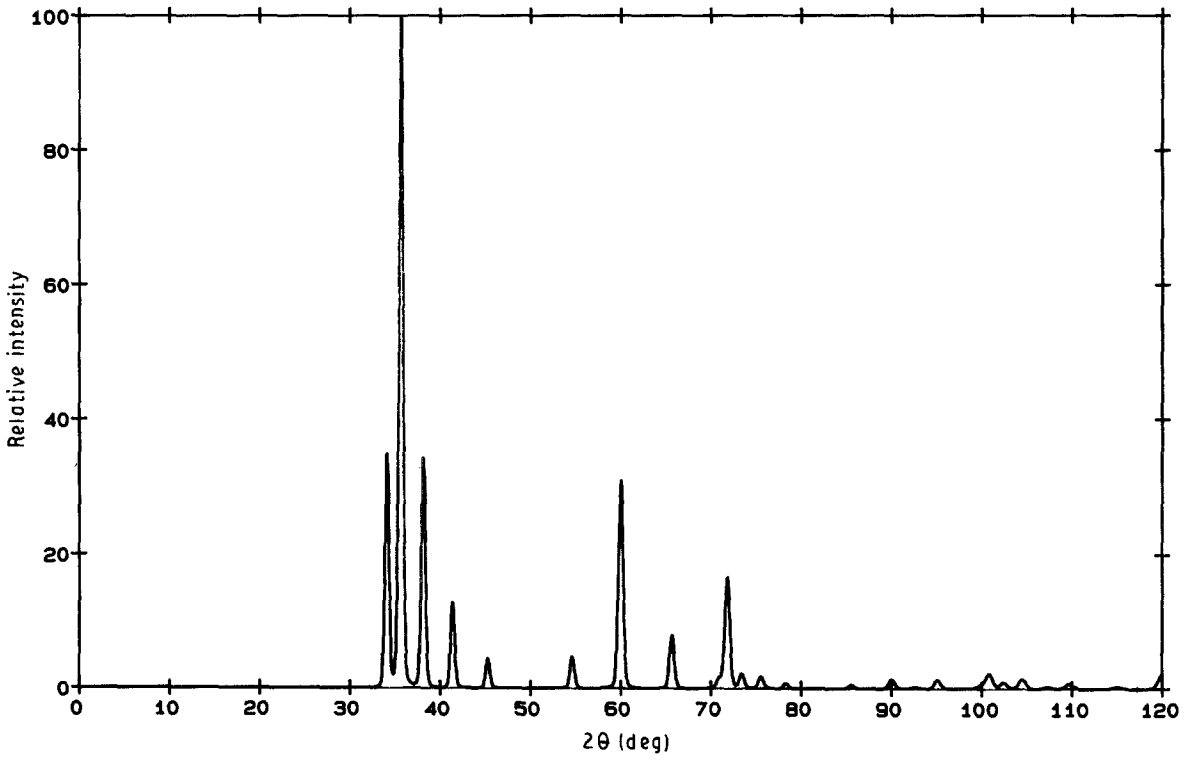

Figure 9 Calculated X-ray diffraction pattern for SiC(6H), mean crystallite diameter 30 nm.

analysis:

Total silicon	69.11 (wt %)
Total carbon	29.12
Free carbon	0.09
Silicon carbide (assay)	96.86
Iron	0.45
Aluminium	0.23
Titanium	0.025
Zirconium	0.027
Calcium	0.03
Magnesium	0.02

The sum of the above elemental percentages amounts to 99.01 wt %. It is likely that oxygen and/or nitrogen make up the balance of the elemental composition. A well comingled mixture of 0.16884 g of NBS SiC-standard and 0.01226 g of hyperpure Si powder

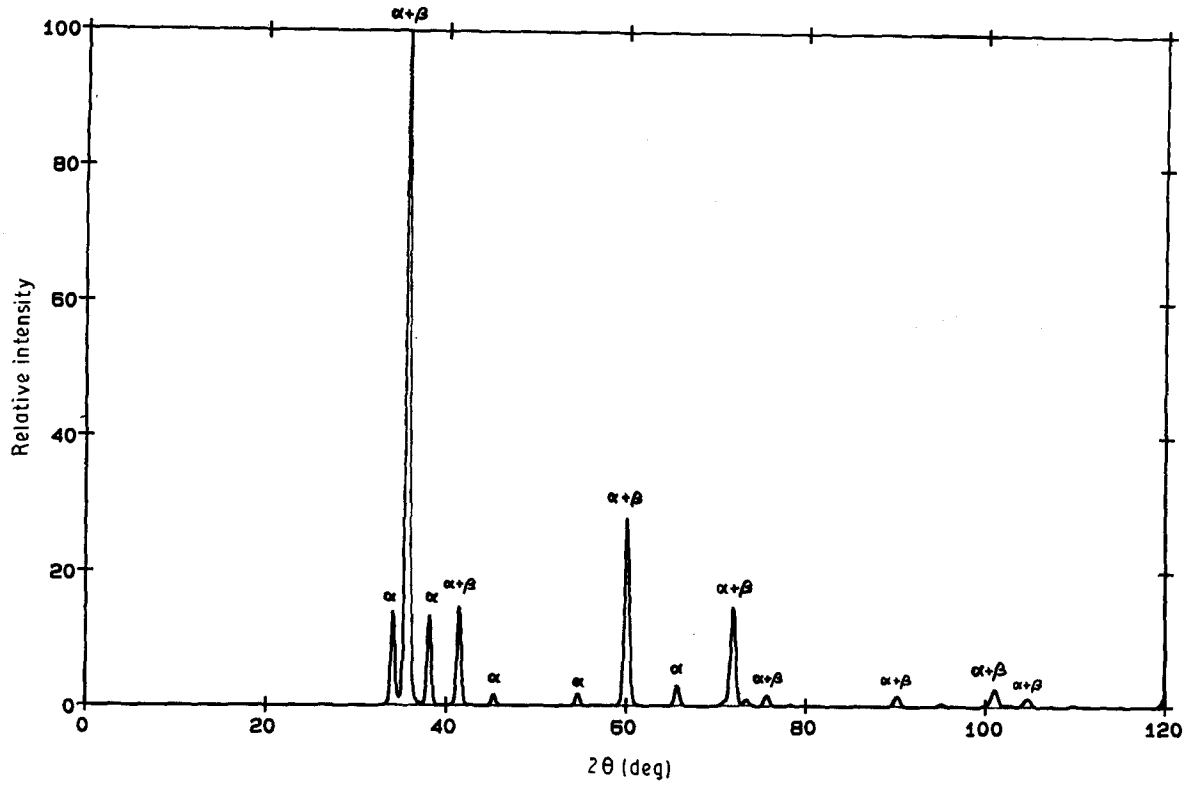

Figure 10 Calculated X-ray diffraction pattern for a 50/50 mixture of SiC(6H) and SiC(3C), called α and β, respectively, each with mean crystallite diameter 30 nm.

TABLE VIII Peaks obtained with Cu$K\alpha$ radiation

SiC polytype	Number of peaks 30 to 45° (2θ)	Unresolved peaks (nm)
β (3C)	2	
2H	3	
4H	5	
6H	5	0.2520, 0.2157
8H	7	0.2660, 0.2643
15R	8	0.2660, 0.2640; 0.2518, 0.2515
21R	11	0.2663, 0.2653; 0.2518, 0.2515
33R	12	0.2645, 0.2633; 0.2602, 0.2583, 0.2539, 0.2518, 0.2515
3 ∞ R	∞	0.267 . . . 0.2518

(325 mesh, as internal standard) was prepared in a boron carbide mortar; of this mixture 0.085 g was loaded into a sample holder having a cylindrical cavity (13 mm diameter and 0.20 mm depth). Columns 1–3 of Table X reproduce the experimental diffraction data. Columns 4 and 5 show the matched *d*-spacings for polytype SiC(6H) and the corresponding matched intensities. Columns 6 and 7 give the assignments for the 15R polytype. For the 4H polytype, two assignments were made to compare the agreement of the calculated data with the experimental data. The respective scale factors for converting relative intensities to the values for I_s (columns 5, 7, 9 and 11) are 1.103, 0.095, 0.103, and 0.105. From the quotient $\Sigma I_s(\text{SiC(6H)})/\Sigma I_v(\text{SiC}) = 338.4/423.8$, we obtain the weight percentage of SiC(6H) as 79.8%. Likewise for SiC(15R) the quotient 38.3/423.8 yields 9.0 wt%. Two values are obtained for ΣI_s (SiC(4H)); namely 47.9 (for the reference pattern 22–1317) and 45.1 for the calculated pattern. The respective values are 11.3 and 10.6 wt % SiC(4H). The polytype composition is therefore reported as 80.0 wt% SiC(6H), 9.0% SiC(15R) and 11.0% SiC(4H). The faint, unidentified lines (0.1902, 0.1594 nm) reveal the presence of at least one minor impurity phase. The more recently issued standard SiC (SRM 112b) also shows this impurity.

A third sample of a SiC standard (Hermann C. Starck A10) was analysed for polytypes. Table XI contains the experimental data, $\{d_v, I_v\}$, and the matched data for SiC(6H) and SiC(15R). From the quotients 263/303 and 33/303, we obtain 87.0 wt% SiC(6H) and 11.0 wt% SiC(15R). The sum, 98%, indicates that the absolute value for SiC(6H) could be off by ± 2% or that a minor concentration of SiC(4H) was not detected.

Fig. 11 shows the diffractogram of Ibiden Betarundum, a commercially available β-SiC. The descending background from 33.6°(2θ) to 40° (2θ) is typical of a disordered SiC structure. The pseudo-triangular area (above true background) divided by the total integrated diffractogram (above background) expresses the volume fraction of disordered β-phase [6]. Table XII gives the experimental diffraction data for the Betarundum. The small peak at 0.2663 nm could be assigned to SiC(2H), (4H) or (8H). However, since no peak was observed at 0.2579 nm nor at 0.2478 nm, the non-β SiC phase was designated as SiC(2H). For a disordered SiC, the above-described method of calculating weight percentages results in too low a value for the β-SiC phase (89.4%). Since the total sample corresponds chemically to SiC, and since there is no morphological (TEM) evidence for a separate macroscopic disordered phase, one best expresses the

TABLE IX Phase identification of SiC (Cerac pure).

SiC (Cerac Pure lot 1587)		SiC(6H) PDF 29-1131			SiC(6H) calculated		SiC(15R) PDF 22-1301			SiC(15R) calculated		
d_v^a (nm)	I_v^b (nm)	d_s (nm)	I_s	hkl	d_s (nm)	$(I_s)_p^c$	d_s (nm)	I_s	hkl	d_s (nm)	$(I_s)_p$	I_v-$\Sigma(I_s)_p$ p
0.2730	1											1
0.2666	2						0.266	2.5	101, 012	0.2660	3.4	− 0.5
0.2632	45	0.2621	43	101	0.2628	41				0.2640		2.0
0.2574	6						0.258	5.1	104	0.2566	6.4	0.9
0.2521	130	0.2511	125	102, 006	0.2518	125	0.251	5.1	00·15, 015	0.2518	9.2	− 0.1
0.2398	5						0.240	4.5	107	0.2391	4.7	0.3
0.2361	45	0.2352	43	103	0.2359	46						2.0
0.2326	4						0.232	3.8	018	0.2322	3.4	0.2
0.2180	18	0.2174	17	104	0.2180	19	0.219	0.6	1·0·10	0.2178	0.6	0.4
0.2105	1						0.211	1.9		0.2106	1.1	− 0.9
0.1999	7			105	0.2001	7.5						− 0.5
0.1968	1						0.197	0.6		0.1965	0.4	0.4
0.1706	1						0.170	1.3	0·1·17	0.1708	0.6	− 0.3
0.1678	10			107	0.1679	8.8						1.2
0.1610	1											1
0.1596	3						0.159	3.8	0·1·19	0.1594	1.7	− 0.8
0.1540	75	0.1537	72	110, 108	0.1541	65	0.154	6.4	110, 0·1·20	0.1540	6.5	− 3.4
0.1505	1											1
0.1445	4						0.1444	3.8		0.1444	2.0	0.2
0.1420	20	0.1418	19	109	0.14216	18						1.0
0.1398	3						0.1398	2.5		0.1398	1.6	0.5
0.1330	5			201	0.13292	6						− 1.0
0.1325	1						0.1320	1.3		0.1318	1.0	− 0.3
0.1314	52	0.1311	50	116, 202	0.1315	41	0.1311	5.7	1·1·15, 205	0.1314	4.5	− 3.7
0.1290	8	0.1286	(19)	203	0.1290	6.3	0.1297	1.3	027	0.1294	0.6	0.4
0.1288	2						0.1281	1.3	028, 0·1·26	0.1280	1.0	0.7
0.1260	6	0.1256	7	0·0·12, 204	0.1257	5	0.1257	1.3	0·0·30, 0·2·10	0.1258	1.0	− 2.3

[a] d_v = Observed interplanar spacings.
[b] I_v = Corresponding peak intensity.
[c] $(I_s)_p$ = Calculated peak intensity.

TABLE X Phase identification of SiC (NBS 112)

SiC (NBS 112)			SiC(6H)		SiC(15R)		PDF 22-1317 SiC(4H)		Calculated pattern SiC(4H)	
$2\theta_v$ (deg)	d_v (nm)	I_v	d_s (nm)	I_s	d_s (nm)	I_s	d_s (nm)	$(I_s)_{obs}$	d_{calc} (nm)	I_{calc}
33.53	0.2673	3.6			0.2660	0.7	0.2661	2.1	0.2669	2.6
34.07	0.2632	42.6	0.2628	36.4	0.2640	2.6				
34.73	0.2583	4					0.2573	10.3	0.2579	10.5
34.93	0.2569	8			0.2566	6.7				
35.61	0.2521	13.0	0.2518	110.3	0.2518	9.5	0.2513	8.2	0.2515	6.8
37.57	0.2394	4.3			0.2391	4.7				
38.13	0.2360	36	0.2359	40.8			0.2352	9.3	0.2357	9.9
38.73	0.2325	3			0.2322	3.2				
41.37	0.2183	13.8	0.2180	16.5	0.2178	0.7				
42.83	0.2111	1			0.2106	1.0				
43.29	0.2090	1.5					0.2084	2.6	0.2088	1.7
45.33	0.2001	8.8	0.2001	6.6						
47.85	0.1901	3								
53.53	0.1712	2			0.1708	0.4				
54.65	0.1679	7.2	0.1679	7.7						
57.25	0.1609	5					0.1604	3.1	0.1607	2.1
57.85	0.1594	1			0.1594	1.0				
60.09	0.1540	44.4	0.1541	57.3	0.1540	3.8	0.1537	4.6	0.1541	4.9
60.89α_1	0.1520	4.3 × 1.5								
64.45α_1	0.1445	6.4 × 1.5			0.1444	1.0				
65.65α_1	0.1421	22 × 1.5	0.14216	15.4			0.1418	4.1	0.1420	3.4
66.81α_1	0.1399	3 × 1.5			0.1399	0.8				
70.85α_1	0.1329	8 × 1.5	0.13293	11.0						
71.87α_1	0.1315	43	0.1315	36.4	0.1314	2.2	0.1311	3.6	0.1314	3.2

The sum of the intensities of Cu$K\alpha_1$ + Cu$K\alpha_2$ are expressed as $I\alpha_1 \times 1.5$

TABLE XI Phase identification of Starck silicon carbide (Starck A10) + 9.59 wt % Si°

		Si°		SiC(6H)		SiC(15R)		
d_v (nm)	I_v	d_s (nm)	I_s	d_s (nm)	I_s	d_s (nm)	I_s	$I_v - \Sigma(I_s)_1$
0.3133	31.2	0.3136	31	–	–	–	–	0.2
0.2630	35			0.2628	29.2	0.2644	2.8	3.0
0.2569	6.5					0.2566	5.8	0.7
0.2520	110			0.2518	88.4	0.2518	8.1	13.5
0.2392	2					0.2391	4.0	– 2.0
0.2359	31			0.2359	32.7			– 1.7
0.2328	2					0.2322	2.8	– 0.8
0.2179	11			0.2180	13.3	0.2178	0.6	– 2.9
0.2107	1					0.2106	0.9	0.1
0.2001	5			0.2001	5.3			– 0.3
0.1921	19	0.1920	18					
0.1706	1					0.1708	0.3	0.7
0.1677	5.5			0.1679	6.2			– 0.7
0.1638	10	0.16387	11					– 1.0
0.1610	1							
0.1595	1.5					0.1594	0.9	0.6
0.1541	45			0.1541	46.0	0.1540	3.3	– 4.3
0.1444	2					0.1444	0.9	1.1
0.1421	12			0.1422	12.4			– 0.4
0.1402	1					0.1399	0.7	0.3
0.1359	2.5	0.1358	2.4					0.1
0.1329	2			0.1329	0.5			1.5
0.1316	29			0.1315	29.2	0.1314	1.9	– 2.1
ΣI_v (SiC) = 303				ΣI_s = 263.2		ΣI_s = 33		
				87%		11%		

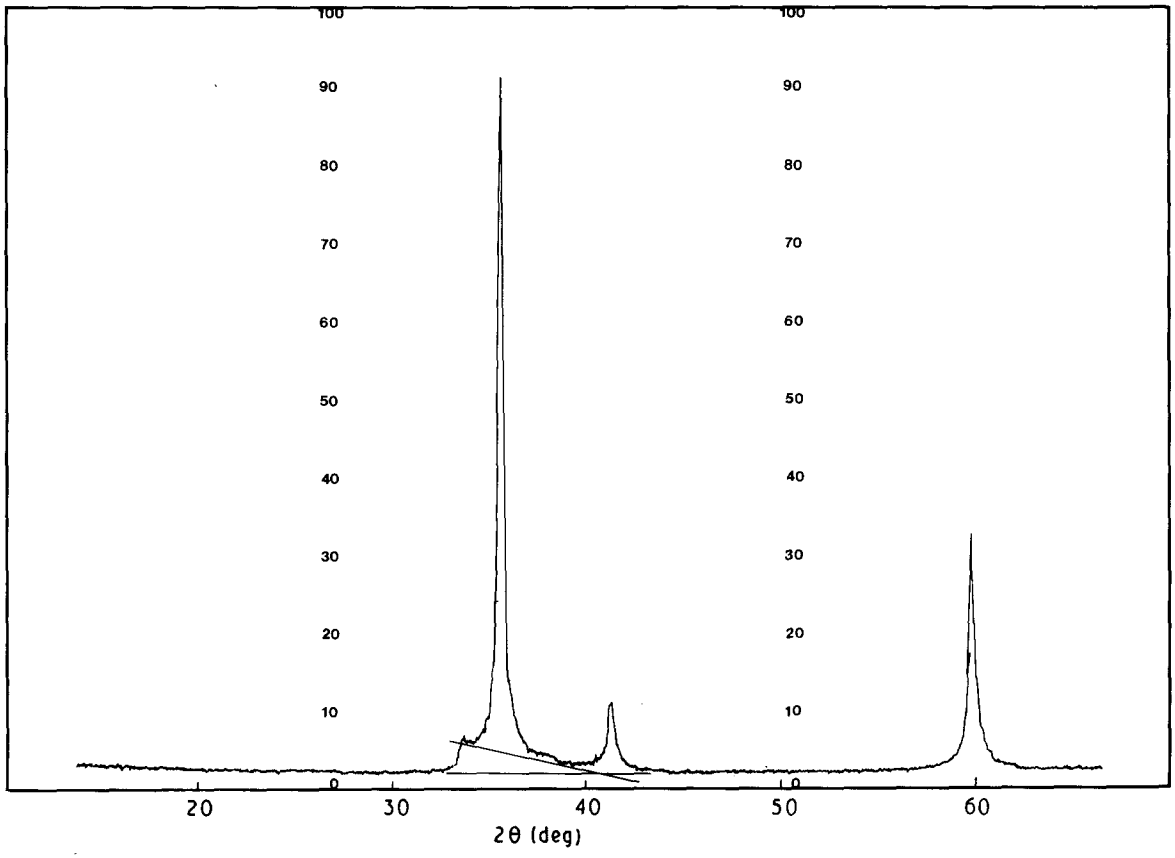

Figure 11 Observed X-ray diffraction pattern for a commercial silicon carbide, predominantly SiC(3C), showing a broad feature due to disorder, 33 to 40° (2θ).

amount of β-SiC phase as 96 ± 2% with a 30% disorder (after [6]). The authors have examined also three commercial SiC whiskers showing varying degrees of disorder (see Table XIII). It is to be noted that with an increase in the disorder index, there is concomitant increase in the relative intensities of the 2 2 0 and 3 1 1 reflections and a decrease in the 2 0 0 reflection. Further studies will be required to correlate the observed diffraction profiles with the atomic arrangements in the disordered submicroscopic regions.

TABLE XII Phase identification of Betarundum (SiC)

	SiC(2H)			β-SiC (total)		β-SiC (ordered)
d_v (nm)	I_v	d_s (nm)	I_s	d_s (nm)	$I_v - I_s$(2H)	I_s(3C)
0.2663	2	0.2668	2			
0.2520	100	0.2515	1.3	0.2517	98.7	82.9
0.2378	1 (broad)	0.2357	2.5			
0.2175	10.7			0.2180	10.7	15.7
0.1540	36.7	0.1541	0.9	0.1541	35.8	35.6
0.1313	25.5	0.1314	0.6	0.1314	24.9	22.4
0.1255	3.3	0.1258	0.1	0.1258	3.2	3.3
	$\Sigma = 179$		$\Sigma = 7.4$		$\Sigma = 173.3$	$\Sigma = 159.9$
	v		(2H)		β	(3C)
			4.1%		96.6%	89.4%

Ratio of triangular area to total integrated intensity (area) above background is 0.32.

TABLE XIII Comparison of relative intensities of X-ray diffraction peaks for β-SiC whiskers

	PDF 29-1129		β-SiC		Tokai		Am. Matrix		Tateho	
$(hkl)^a$	d_{obs} (nm)	$(I/I)_{obs}$	d_{calc} (nm)	$(I/I)_{calc}$	d_{obs} (nm)	$(I/I)_{obs}$	d_{obs} (nm)	$(I/I_1)_{obs}$	d_{obs} (nm)	$(I/I_1)_{obs}$
111	0.252	1.00	0.2517	1.00	0.252	1.00	0.2516	1.00	0.2527	1.00
200	0.218	0.20	0.2180	0.19	0.218	0.16	0.2175	0.10	0.2187	0.06
220	0.1541	0.35	0.15412	0.43	0.1542	0.43	0.1540	0.62	0.1545	0.77
311	0.13140	0.25	0.13144	0.27	0.1315	0.29	0.1313	0.40	0.1318	0.39

[a] hkl = indices of reflection for the cubic polytype of SiC.
The standard pattern for β-SiC is given in columns 2 and 3; the calculated pattern is based on the 2,2F$\bar{4}$3m(4) structure and a lattice constant of $a = 0.43593(6)$ nm. The empirical disorder index for the above SiC whiskers is 0.033, 0.095, and 0.187, respectively, with the larger values indicating greater disorder.

In over 300 samples of SiC analysed, the authors have encountered only the polytypes β-SiC(3C), SiC(6H), SiC(15R), SiC(4H), and occasionally SiC(2H) and SiC(8H). When the SiC samples are well crystallized and exhibit a low degree of stacking faults, the weight percentages of the various polytypes can be determined within 5–10% of the actual amount present; the limit of detection is about 2 – 5 wt%.

4. Other measurements of SiC polytypes

Several ways of interpreting the powder diffraction pattern of a SiC multiphase mixture to give the quantitative phase distribution have been described. Jagodzinski and Arnold [6] describe a procedure based on the preparation of physical mixtures of pure SiC(3C) with impure SiC(6H), that is, with the latter containing an unknown fraction of SiC(3C). Calculated intensities for the two phases are found, and pairs of observed diffraction maxima from several mixtures are used to determine the composition of the impure component. This assumes that only two phases are present. The extension of this method to a three-phase mixture leads to quite involved equations.

Kawamura [7] looks at the three diffraction maxima at 0.263, 0.257, and 0.252 nm, and ascribes them as due to contributions from 6H only, from 15R only, and from 3C + 6H + 15R, respectively. He also calculates intensities for the phases involved, and then solves three equations in three unknowns to establish the three percentage compositions. Note that 4H is specifically excluded from his procedure, even though the diffraction pattern which he shows has an obvious maximum at 0.267 nm due to 4H.

Balloffet *et al.* [8] prepared known mixtures of 3C, 6H, and 4H and plotted the relative intensity ratios of selected maxima as functions of the 6H and 4H concentrations to establish calibration curves. Bartram [9] concludes that the considerable difference in the results obtained from two different peak ratios, and the neglect of the possible presence of other polytypes makes this method inadequate. Bartram [9] extended the method of Kawamura [7] by using six relatively prominent peaks in the range from 0.267 to 0.218 nm to establish the fractional contributions of the four polytypes 3C, 6H, 4H and 15R. While he has limited his analytical treatment arbitrarily to these four phases, he clearly indicates that the method can be extended to include others. He calculates unitary structure factors for the several reflections of each polytype, uses the appropriate multiplicity factors, the product of the Lorentz and polarization factors, L_p, and finds the normalized integrated intensity values presented in Table XIV. The final numerical column puts all of the normalized intensity data on a scale of 100 for comparison. Note that the two minor 15R maxima at 0.239 and 0.232 nm are not used in the analysis.

A linear equation is written for each of the six principal maxima using the reduced intensity values

TABLE XIV Normalized integrated intensity values

d (nm)	Phase	F_{unit}	Mult.	L_p	I_{norm}	I_{red}	Peak
0.2669	4H	3.30	66	21.1	1380	9.52	A
0.2660	15R	1.88	6	21.0	445	3.07	
0.2628	6H	3.53	12	20.6	3080	21.24	B
0.2640	15R	3.56	6	20.5	1560	10.76	
0.2579	4H	4.85	12	19.5	5500	37.93	C
0.2566	15R	5.66	6	19.4	3730	25.72	
0.2518	6H	9.91	2	18.5	3630	25.03	D
0.2518	6H	4.95	12	18.5	5440	37.52	
0.2517	3C	9.90	8	18.5	14500	100.00	
0.2517	15R	9.91	2	18.5	3630	25.03	
0.2515	4H	9.90	2	18.5	3630	25.03	
0.2514	15R	3.94	6	18.5	1720	11.86	
0.2391	15R	5.23	6	16.5	2710	18.69	
0.2357	4H	5.28	12	15.9	5320	36.69	E
0.2359	6H	4.08	12	15.9	3180	21.93	
0.2322	15R	4.46	6	15.4	1920	13.24	
0.2180	3C	5.62	6	13.3	2520	17.38	F
0.2180	6H	2.78	12	13.3	1235	8.52	
0.2178	15R	2.27	6	13.3	410	2.83	

for the polytypes which contribute. Thus:

(nm)	15R	6H	4H	3C	Peak
0.267	$3.07a +$	$0.00b +$	$9.52c +$	$0.00d = A$	(1)
0.263	$10.76a +$	$21.24b +$	$0.00c +$	$0.00d = B$	(2)
0.257	$25.72a +$	$0.00b +$	$37.93c +$	$0.00d = C$	(3)
0.252	$36.90a +$	$62.55b +$	$25.03c +$	$100.00d = D$	(4)
0.236	$0.00a +$	$21.93b +$	$36.69c +$	$0.00d = E$	(5)
0.218	$2.83a +$	$8.53b +$	$0.00c +$	$17.38d = F$	(6)

with a–d being the relative fractions of 15R, 6H, 4H, and 3C, respectively. The measured values of the integrated intensities are substituted for A–F and the resulting six equations solved for the four unknowns a–d by multiple regression (least-squares reduction). Subsequently, these relative fractions are scaled so that $a + b + c + d = 100\%$.

Ruska *et al.* [10] used substantially the same procedure to develop a similar set of equations. In this case, experimental observations of the peak intensity ratios of mixtures of SiC(3C) and SiC(6H) were used to modify the coefficients, giving the equation set:

$$3.19a + 0.00b + 9.88c + 0.00d = A \quad (7)$$
$$11.17a + 19.40b + 0.00c + 0.00d = B \quad (8)$$
$$25.99a + 0.00b + 38.90c + 0.00d = C \quad (9)$$
$$37.05a + 59.20b + 25.09c + 100.00d = D \quad (10)$$
$$0.00a + 18.10b + 36.06c + 0.00d = E \quad (11)$$
$$2.41a + 6.50b + 0.00c + 13.10d = F \quad (12)$$

To test the method of Ruska *et al.* [10], we prepared a finely ground specimen of SiC (SRM 112b) and made eight separate sample mountings, taking pains to minimize preferred orientation. These samples were run using CuKα radiation at 40 kV and 20 mA in a Philips vertical diffractometer fitted with a graphite monochromator. The scan rate was $0.25° \text{ min}^{-1}$ and the counter time constant 2 s. A sample spinner was used. The patterns were recorded on chart paper, and peak areas subsequently measured using a planimeter. These areas were used as the values A–F in Ruska's equation set. The equations were solved by multiple regression analysis, and the resulting relative fractions normalized (Table XV).

The arithmetical mean values are here unweighted, and the numbers in parentheses are 1 standard deviation, also unweighted. The polytype distribution for this sample by the authors' method was determined as 8(3)% SiC(15R), 51(2)% SiC(6H), 41(5)% SiC(4H), and nil(1)% SiC(3C).

From the eight separate runs, it can be stated that the spread in the results (-3.9–11.3% for 15R; 45.4–59% for 6H; 33.6–49.8% for 4H; and -0.9–14.8% for 3C) casts serious doubt on the accuracy/validity of the phase determination of polytypes at low (< 5 wt%) concentrations. The reason for this shortcoming is the high sensitivity of the method of simultaneous equations to moderate fluctuations in the intensities of the six strongest reflections. By contrast, the method practiced here uses the characteristic weak, non-overlapping reflections of a particular non-cubic polytype to determine its concentration independently. For low (< 5 wt%) concentrations of β-SiC, it is advisable to confirm its presence by examining the powder sample in polarized light if the isotropic particles are greater than 1 μm or preferably by electron diffraction of single sub-micrometre particles to confirm their cubic symmetry.

TABLE XV Solutions to Ruska *et al.*'s [10] equation set—normalized relative fractions

Run	15R (%)	6H (%)	4H (%)	3C (%)
1	11.32 (7.30)	50.72 (6.29)	32.59 (4.22)	5.36 (4.30)
2	3.57 (2.27)	51.18 (1.95)	39.80 (1.31)	5.46 (1.33)
3	4.09 (2.96)	49.39 (2.55)	40.38 (1.71)	6.13 (1.74)
4	− 3.90 (15.66)	55.36 (13.49)	49.76 (9.06)	− 0.93 (9.21)
5	6.68 (6.73)	45.36 (5.80)	33.18 (3.89)	14.79 (3.96)
6	2.07 (3.79)	55.17 (3.27)	37.34 (2.19)	5.42 (2.23)
7	9.31 (4.11)	49.98 (3.54)	33.68 (2.38)	7.04 (2.42)
8	− 2.43 (6.35)	58.95 (5.47)	42.63 (3.67)	0.84 (3.74)
Mean	3.84 (5.30)	52.01 (4.26)	38.67 (5.81)	5.51 (4.66)

Acknowledgement

The authors are grateful to Cyrus Crowder of the Dow Chemical Company for generating with POWD12 the calculated powder patterns of the various SiC polytypes.

References

1. R. G. W. WYCKOFF, "Crystal structures", Vol. 1, 2nd edn, (Interscience, New York, NY, 1963) p. 113.
2. D. K. SMITH and K. L. SMITH, "POWD12: A FORTRAN 77 program for calculating X-ray powder diffraction patterns", Pennsylvania State University 1986.
3. L. LANDAU, *Phys. Zeits. Soviet Union* **12** (1937) 569.
4. I. M. LIFSCHITZ, *ibid.* **12** (1937) 623.
5. S. HENDRICKS and E. TELLER, *J. Chem. Phys.* **10** (1942) 147.
6. M. JAGODZINSKI, and H. ARNOLD, in Proceedings of the Conference on Silicon Carbide, Boston, Massachussetts, April 1959, edited by J. R. O'Conner and J. Smittens (Pergamon, New York, 1960), p. 130.
7. T. KAWAMURA, *Mineralog. J.* **4** (1965) 333.
8. Y. BALLOFFET, *et al.* Report AECL-3673 (Whiteshell Nuclear Research Establishment, Pinawa, Manitoba, Canada, 1971).
9. S. F. BARTRAM, "Quantitative Analysis of SiC Polytypes by X-ray Diffraction", Technical Report 75CRD022 (General Electric Company, Schenectady, NY, 1975).
10. J. RUSKA, L. J. GAUCKLER, J. LORENZ and H. U. REXER, *J. Mater. Sci.* **14** (1979) 2013.
11. L. K. FREVEL, *Acta Cryst.* **B41** (1985) 304.
12. R. F. ADAMSKY and K. M. MERZ, *Z. Krist.* **111** (1959) 350.

Received 10 December 1990
and accepted 13 May 1991